



## Research Article

# Mathematical modelling of evaporation rate and heating of biodiesel blends of a single-component droplets

Madan BASNET<sup>1</sup>, D. SENTHILKUMAR<sup>1</sup>, R. YUVARAJ<sup>1,\*</sup>

<sup>1</sup>Department of Mechanical Engineering, Sonacollege of Technology, Salem, Tamilnadu, 636005, India

## ARTICLE INFO

### Article history

Received: 28 April 2021

Revised: 04 January 2022

Accepted: 05 February 2022

### Keywords:

Single Droplet Experimental Setup; Single Component Biodiesel Droplet; Evaporation Rate; Combustion Performance

## ABSTRACT

Biodiesel serve as promising fuel and optimal alternative for mitigating the present issues of fuel scarcity and emission control in compression ignition engines. Several Researches have concluded that engine performance and its emission characteristics heavily depends on parameters like fuel droplet spray formation, atomization, evaporation and combustion which in turn depend on thermophysical properties of biodiesel fuel. In this study, the thermophysical properties like normal boiling, critical properties, vapor pressure, latent heat of vaporization, liquid density, liquid viscosity, liquid thermal conductivity, gas diffusion coefficients of two biodiesel fuels sample: Madhuca Indica and Radish oil are determined using standard correlation. Accurate mathematical model for estimation of evaporation rate and combustion of single component biodiesel droplet is framed and validated with single droplet setup experiment result for Jatropa Methyl Ester (JME), Karanja Methyl Ester (KME), Mahua Methyl Ester (MME), Neem Methyl Ester (NME), Palm Methyl Ester (PME) oil and this model is further extrapolated to predict the evaporation and combustion behaviour of two unexperimented oil, Madhuca and Radish.

It is found that Madhuca oil has the higher evaporation constant value of 0.1466 mm<sup>2</sup>/s and thus lowest lifetime in among the biodiesel fuel studied. This value is attributed to lower molecular weight and higher molecular diffusivity. On the other hand reverse trend is observed in Radish with lower evaporation constant and higher lifetime. This study behaves as comprehensive methodology for estimating the behaviour of biodiesel based on their composition and chemical structure and also as firm framework for combustion modelling in enhancing engine performance.

**Cite this article as:** Basnet M, Senthilkumar D, Yuvaraj R. Mathematical modelling of evaporation rate and heating of biodiesel blends of a single-component droplets. J Ther Eng 2023;9(6):1572–1584.

### \*Corresponding author.

\*E-mail address: [yuvarajr@sonatech.ac.in](mailto:yuvarajr@sonatech.ac.in)

*This paper was recommended for publication in revised form by Regional Editor Nader Javani*



## INTRODUCTION

Scarce availability of petroleum and diesel has diverted people attention and concern towards biodiesel. Fossil fuel over-drainage, its exponential price hike & global warming are alarming issues in the contemporary machine world pertaining to the energy crisis and ecological imbalance. The biodiesel fuel being multi-component retaining single component characteristics, its renewable nature, its high applicability band within the conventional IC engine with minor modifications, and when used after emulsified and blended with additives alleviates the shortcomings owing to the high volatility, better ignition quality, energy and mass density, higher safety, non-toxic in nature. The applicability of biodiesel encompasses farm automobiles, power stations as well as heavy vehicles in this era. Biodiesel fuel derived from vegetable seeds and animal fats are the best alternative fuel for compression ignition engine operating with or without modification. and possess numerous merits of superior emission characteristics, cost effectiveness for mass production, renewable nature, easy storage and better lubrication. Several benefits of vegetable biodiesel are low CO<sub>2</sub> consumption, reduced pollution, maximum yield, production from waste biomass, renewable nature, sustainability, cultivable throughout the year, food-friendly, and engine applicable. In terms of emission researchers have shown that use of biodiesel has substantial reduction in the unburnt hydro-carbon (HC), Particulate matter (PM) and Carbon monoxide emissions (CO) even though slight increment in Nitrogen Oxide (NO<sub>x</sub>) emission is obtained [1–4]. The assessment of thermophysical nature and the rate of bio-diesel vaporization with five biodiesels samples were carried out in single droplet setup experiment [5]. A Comparison of fully transient (FT) and Quasi steady (QS) approaches employed to study multi droplet evaporation indicates amount of heavier components of droplet composition and increasing volatility differences of components increases the deviation of two approaches [6]. Numerical Simulation of single droplet with infinite conductivity model was conducted by researchers under low pressure (0.1Mpa) with various temperature range (550-1050K) to obtain temporal evolution of droplet diameter squared, droplet surface temperature and average evaporation rate of Rapeseed Methyl Ester (RME) and Sunflower Methyl Ester (SME) [7]. Compared to gasoline and diesel droplets the biodiesel droplet's evaporation rate and surface temperature are higher and also it is higher for the multi-component model than the single-component model i.e., the boiling point of the heavier components in the droplet is high. Discrete Component (DC) model is applied taking temperature gradient, recirculation and species conservation for heating and evaporation of multi component droplet [8]. The presence of additional O<sub>2</sub> atoms, makes the carbon atoms get oxidized to a higher level which results in minimizing the Carbon monoxide emission, this process of oxidation requires a complicated chemical method. Spray

combustion entails spray process, droplet size and heating which helps to reduce the detailed methodology of the process and to look into the ignition and emission development/oxidation of the test engine with 3D simulations [9]. Among the three spray model CAB (Cascade Atomization and Dropbreak) and ETAB models better predicted the tip penetration of fuel vapour than KH RT (Kelvin Helmholtz and Rayleigh Taylor) model against Experimental Data [10].

### Biodiesel Droplet Modeling

The multi-dimensional quasi discrete model is used to model the evaporation rate and heating of dual fuel droplets for a specific use of soybean biodiesel with diesel blends as a diesel engine fuel [11]. Ethanol/Petroleum fuel droplets' evaporation or combustion characteristics has been investigated [12]. Droplet evaporation characteristics are reported using the activity coefficient and continuous thermodynamics method [13]. Using continuous mixture theory, a model is generated used to find the evaporation rate of biodiesel droplets and is validated with a single suspended droplet experimental setup [14]. The analysis of Rapeseed Methyl Ester and Sunflower Methyl Ester was carried out at the realistic temperature of range 473K to 1020K at atmospheric pressure and the comparison of newly obtained results and former results of n-alkanes was done based on the prediction from quasi-steady theory [15]. The vegetable oil's steaming nature can be forecasted by comparing on hand model with the newly obtained results. The theoretical quasi steady model based on determination of transport and thermodynamic properties is used for predicting evaporation characteristics of cotton seed oil using the properties of its predominant Fatty Acids (linoleic, oleic and palmitic) [16]. In increased temperature surroundings, the steaming nature of Palm Methyl Ester drop is studied by conducting a test called droplet vaporization test in a hot chamber. A Thermo Gravimetric-Differential Thermal (TG-DT) analysis is carried out to look into the existence of exothermic reactions [17]. A better quantitative model has been put forward to analyze the nature of rapeseed methyl esters and sunflower methyl esters droplets, under realistic pressure and temperature. And then they are combined with thermo-physical properties to build a base for upcoming spray ignition simulations [7]. An equation is framed in such a way that it suits all cases to describe the droplet radius concerning time. The two prime models are given, out of which one deals with the real work of Maxwell which states that mass diffusion in vapour is paramount as rate limiting step for evaporation than the heat movement across vapor. The kinetic correction occurs when there is a temperature jump at the interface which affects the momentum/pressure equilibrium [18]. A mathematical correlation was aimed to build between the biodiesel nature and fuel temperature and this equation has been planned to use for examining the temperature effect on certain characteristics of fuel like performance, emissions, and combustion of the engine with

four biodiesel samples which were analyzed in accordance to the Indian biodiesel standard and the European biodiesel standard. Testing was done on the biodiesel in the absence of nitrogen and non-adding of antioxidants for about half a year, to simulate typical fieldwork. This fails to achieve the oxidation stability criterion and required the use of anti-oxidants in the field [19].

The complexity indulged are meagre thermophysical data and correlations available for the analytical and experimental study. The decomposition during storage, bond dissociation, isomeric interchangeability and poly-unsaturated ester causing high viscosity, lower volatility, and poor oxidative range are hurdles. The problems are rectified using transference, emulsification and blending respectively.

Above survey from researcher studies and authors' knowledge, many studies were carried out with different models to find the evaporation rate and surface temperature of different droplets. Very little work was done due to challenges in the determination of thermo-physical properties, its tediousness and its cumbersome nature. A complete model that estimates and predetermines the evaporation seems lagging. This study concentrates on single component mathematical modeling to find and analyze the various properties and evaporation.

## MATHEMATICAL MODELLING

### Assumptions

The assumptions made in our study of droplet evaporation are: I. Initially, the mass transfer coefficient is less than the heat transfer coefficient so the droplet diameter increases in the expansion phase (dilation). Afterward, the heat transfer coefficient dominates and a decrease in diameter occurs in the transient heating phase till the equilibrium (steady) phase is reached. In the steady phase, the heat transfer coefficient is exactly equal to the mass transfer coefficient. II. Droplet evaporates in a quiescent infinite medium. III. Evaporation is quasi-steady. IV. Droplet temperature is assumed to be uniform. V. The Stephan problem is reduced to a spherically symmetric co-ordinates system. VI. Lewis's number is assumed to be unity. VII. Thermo-physical properties like thermal conductivity, density, specific heat, etc. are assumed to be constant [20].

### Gas-phase Analysis

#### Transient heating time (Heat and mass conservation)

Chin and Lefebvre developed a method to determine the transient heating time. Before the assumption of thermal balance of the droplet neglecting the radiation heat loss, the assumption of the equivalent diameter of droplet heating lifetime appears to be more prominent [15].

$$t_{h2} = \frac{C_{pl}\rho_l C_{pg} d_h^2 (T_s - T_{s0})}{12 \lambda_g \ln(1 + B_{Mh}) L_{vh} \left[ \left( \frac{B_{Th}}{B_{Mh}} \right) - 1 \right]} \quad (1)$$

In Eqn. 1,  $d_h$  is the average droplet diameter during the heating period and the relation of this average droplet diameter  $d_h$  with initial diameter  $d_0$  is given as:

$$d_h = d_0 \left[ 1 + \frac{C_{pl}(T_s - T_{s0})}{2 L_{vh} \left[ \left( \frac{B_{Th}}{B_{Mh}} \right) - 1 \right]} \right]^{-0.5} \quad (2)$$

Where  $B_{Th}$  is the thermal transfer number given by

$$B_{Th} = \frac{Y_{Fs}}{(1 - Y_{Fs})} \quad (3)$$

$B_{Mh}$  is the mass transfer number given by

$$B_{Mh} = \frac{C_{pg}}{L_v} (T_\infty - T_s) \quad (4)$$

$Y_{Fs}$  is the mass fraction of fuel vapor at the droplet surface and  $T_\infty$  is the ambient temperature.

$$Lv = L_{vTnb} \frac{(T_c - T_s)^{0.38}}{(T_c - T_{nb})} \quad (5)$$

#### Gas phase mass conservation equation

We have assumed burning to be a quasi-steady process, therefore, the mass flowrate,  $\dot{m}(r)$  is a constant, independent of radius [20].

$$\dot{m} = \dot{m}_F = \rho v_r 4\pi r^2 = \text{constant} \quad (6)$$

$$\frac{d(\rho v_r r^2)}{dr} = 0 \quad (7)$$

where  $v_r$  is the bulk flow velocity.

#### Gas-phase energy conservation equation

The conservation of energy for an evaporating droplet in the gas phase is given by the Shvab-Zeldovich energy equation [20].

$$\frac{1}{r^2} \frac{d}{dr} \left[ r^2 \left( \rho v_r \int c_p dT - \rho D \frac{d \int c_p dT}{dr} \right) \right] = - \sum h_{f,i} \dot{m} \quad (8)$$

with the assumption of constant properties and unity Lewis number, Eqn. 8 can be written as:

$$\frac{d \left( r^2 \frac{dT}{dx} \right)}{dx} = \frac{\dot{m} C_{pg}}{4\pi K} \frac{dT}{dr} \quad (9)$$

By solving the energy conservation equation applying following boundary condition,

$$\text{Inner region} \begin{cases} T(r_s) = T_s \\ T(r_f) = T_f \end{cases}$$

$$\text{outer region} \begin{cases} T(r_f) = T_f \\ T(r \rightarrow \infty) = T_\infty \end{cases}$$

substituting  $Z_F=Z_I= \frac{C_{pg}}{4\pi K}$ , the temperature distribution equation is obtained as:

$$T(r) = \frac{(T_\infty - T_{nb})e^{(-Z\dot{m}/r_s)} - T_\infty e^{(-Z\dot{m}/r_s)} + T_{nb}}{1 - e^{(-Z\dot{m}/r_s)}} \quad (10)$$

### Droplet gas-phase interface energy balance

The temperature distribution equation allows us to evaluate the heat transferred to the droplet surface which appears in the interface (surface) energy balance. The layer of hot gas surrounding the droplet conducts heat to the interface. As the droplet temperature is uniform at  $T_{boil}$  the heat supplied will be used to vaporize the droplet without increasing the droplet temperature [20].

The surface energy balance can be written as:

$$\dot{Q}_{cond} = \dot{m}(h_{vap} - h_{liq}) = \dot{m}h_{fg} \quad (11)$$

Differentiating the temperature distribution equation and substituting in above equation the temperature gradient value at the droplet interface is:

$$\frac{dT}{dr} = \frac{Z\dot{m}}{r_1^2} \left[ \frac{(T_\infty - T_{boil})e^{(-Z\dot{m}/r_1)}}{1 - e^{(-Z\dot{m}/r_s)}} \right] \quad (12)$$

By solving the above 2 equations the mass evaporation rate in the stationary environment is obtained as:

For stationary environment

$$\dot{m} = \frac{4\pi k_g r_s}{C_{pg}} \ln(1 + B_q) \quad (13)$$

For convective environment

$$\dot{m} = \frac{2\pi k_g r_s Nu}{c_{pg}} \ln(1 + B_{o,q}) \quad (14)$$

where Spalding or transfer number is given by:

$$B_q = \frac{C_{pg}(T_\infty - T_{nb})}{h_{fg}} \quad (15)$$

For stationary environment

$$\dot{m} = 2\pi d \rho_l D_{bi} \ln(1 + B_{(0,q)}) \quad (16)$$

For convective environment

$$\dot{m} = \pi d \rho_l D_{bi} Nu \ln(1 + B_{(0,q)}) \quad (17)$$

### Steady-state droplet lifetime

At a steadystate, the reduction in droplet mass is equal to the rate of vaporization.

$$\frac{dm_a}{dt} = -\dot{m} \quad (18)$$

applying the geometrical and boundary condition, the droplet diameter can be expressed as a function of time as follows:

$$\frac{dD^2}{dt} = -\frac{8k_g}{\rho_l C_{pg}} \ln(1 + B_q) \quad (19)$$

The time derivative of the square of the droplet diameter is constant; hence,  $D^2$  varies linearly with the slope  $-\frac{8k_g}{\rho_l C_{pg}} \ln(1 + B_q)$ . This slope is defined to be the evaporation constant.

$$K_{evp,s} = -8D_{bi} \ln(1 + B_q) \quad (20)$$

where  $D_{bi}$  is the binary diffusivity coefficient.

For convective environment

$$K_{evp,s} = \frac{2\dot{m}_{evp,s}}{\pi \rho_l d} \quad (21)$$

For stationary environment

$$K_{evp,s} = \frac{4\dot{m}_{evp,s}}{\pi \rho_l d} \quad (22)$$

$$K = \frac{8k_g}{\rho_l C_{pg}} \ln(1 + B_q) \quad (23)$$

For stationary environment

$$K = \frac{4k_g Nu}{\rho_l C_{pg}} \ln(1 + B_q) \quad (24)$$

Eqn.19 can be integrated by substituting value of K from Eqn. 23 on Eqn. 19 to provide a general relationship expressing the variation of D (or  $D^2$ ) with time:

$$\int_{D_0^2}^{D^2} dD^2 = - \int_0^t K dt \quad (25)$$

Which yields

$$D^2(t) = D_o^2 - Kt \quad (26)$$

Eqn. 23 is the D<sup>2</sup> law for droplet evaporation. From experiments, it's known that D<sup>2</sup> law is applicable after an initial transient period associated with the heating of droplets to near the boiling point [21].

We can find the time taken by droplet of a given initial size to evaporate completely, i.e., the droplet lifetime,  $t_d$ , by letting  $D^2(t_d)=0$ :

$$K_{evp,s} = D_o^2 / K \quad (27)$$

Properties like  $c_{pg}$  and  $k_g$  vary considerably from droplet surface to free stream conditions but in our analysis, we have assumed them to be constant because the radial gradient of those variables is negligible. Following the approach of Law and Williams [22] for burning droplets, the following approximations for  $c_{pg}$  and  $k_g$  are suggested:

$$C_{pg} = C_{pF}(\bar{T}) \quad (28)$$

$$K_g = 0.4k_F(\bar{T}) + 0.6k_\infty(\bar{T}) \quad (29)$$

where the subscript F represents the fuel vapor and  $\bar{T}$  is the average of the fuel boiling point temperature and that of the free stream,

$$\bar{T} = (T_\infty + T_{boil})/2 \quad (30)$$

Variation of the convective environment using different Nusselt number correlations:

Froessling [23] and Ranz and Marshall [24,25] correlation:

$$Nu_1 = 2 + 0.552Re_d^{1/2}Pr_g^{1/3} \quad (31)$$

$$\text{where, } Re_d = \frac{\rho_g U_{rel} d_d}{\mu_g} \text{ and } Pr_g = \frac{\mu_g C_{pg}}{k_g}$$

Clift correlation [26]:

$$Nu_2 = 1 + (1 + Re_d Pr_g)^{1/3} f(Re_d) \quad (32)$$

$$\text{Where } f(Re_d) = \begin{cases} 1 & 0 < Re_d < 1 \\ Re_d^{0.777} & 1 < Re_d < 400 \end{cases}$$

$$0.25 \leq Pr \leq 100$$

Faeth and Lazar correlation [27]:

$$Nu_3 = 2 + 0.552 Re_d^{1/2} Pr_g^{1/3} \left( 1 + \frac{1.232}{Re_d^{1/2} Pr_g^{4/3}} \right)^{-1/2} \quad (33)$$

Haywood correlation [28]:

$$Nu_4 = \frac{2 + 0.87 Re_d^{1/2} Pr_g^{1/3}}{(1 + B_M)^{0.7}} \quad (34)$$

Chiang correlation [29]:

$$Nu_5 = \frac{2 + 0.39 Re_r^{0.54} Pr_g^{0.76}}{(1 + B_M)^{0.557}} \quad (35)$$

$$\text{where, } Re_r = \frac{\rho_g U_{rel} r}{\mu_g}$$

## RESULT AND DISCUSSION

### Methyl Esters Compositions

In this Investigation, Fatty Acid Methyl Ester (FAME) composition ranging from C16 to C20 of Madhuca Indica, Radish oil and Coconut oil is tabulated in Table1 [30–33]. The corresponding mole fraction of each component and the equivalent molar mass of methyl ester were determined and using the empirical formula the equivalent Carbon, Hydrogen and Oxygen content of entire bio-diesel were calculated.

**Table 1.** Composition of FFA of Radish, Madhuca, and Coconut biodiesel

Property	Radish seed oil	Madhuca seed oil	Coconut Oil
<b>Free Fatty acid composition (%)</b>			
(i) Palmitic	6.06	10.2	3.8
(ii) Stearic acid	2.13	8.7	1.26
(iii) Oleic acid	23.87	24.6	10.93
(iv) Linoleic acid	11.44	39.6	5.73
(v) Linolenic acid	6.51	16.3	0

**Table 2.** Calculated diffusivity correspondent CHO and molecular weight of biodiesel

Biodiesel	Dbi(m <sup>2</sup> /s)	C	H	O	MW(Kg/Kmol)
Coconut	1.54043 E-5	13.90415	27.80829	2	226.658
Madhuca	1.4055E-5	18.36355	36.7271	2	289.0897
Radish	1.4315E-5	20.17371841	40.34743682	2	314.4321

**Table 3.** Calculated biodiesel properties

Biodiesel	Density (ρl) (Kg/m <sup>3</sup> )	Kinematic Viscosity (ν) (mm <sup>2</sup> /s)	Thermal conductivity (Kl) (W/mK)	Specific Heat Capacity (CPl) (J/KgK)
Coconut	863.2497	4.05251	0.18791	1382.741
Madhuca	867.7161	6.7677	0.16741	1335.736
Radish	870.6853	6.23368	0.16269	1327.8

**Methyl Ester and its Thermo-Physical Properties**

The fatty acid composition is measured after that single component chemical formula was used to determine the equivalent composition of chemical structure [34–36]. Molecular weight, Binary diffusivity and equivalent carbon, hydrogen, and oxygen are listed in Table 2. Diffusivity values of biodiesel oil are calculated using Fullar et al. correlations in the constant (300K) temperature [37–40]. Determined methyl ester properties values are presented in table 3 .From the table viscosity of tested fuels sample value are calculated to lies between 4 to 6.7 mm<sup>2</sup>/s using Sazhin et al. correlation [41,42]. Madhuca indica methyl ester has the highest viscosity among three tested fuels samples. The evaporation process is not independent of the liquid phase viscosity of the fuel. This viscosity affects the atomization and spray behavior. Generally Spray with a Higher Sauter mean diameter is produced by highly viscous oil in the practical application usage. The densities of the

liquid fuel values are calculated to be 863.25, 867.71, and 870.68 kg/m<sup>3</sup> for coconut, Madhuca, and Radish oil respectively using Sazhin et al. correlation [43–45]. Unlike viscosity, the property density doesnot affect spray formation. Radish biodiesel has a higher density of the fuel ,the reason is because of contribution of Molecular weight. Similarly, Thermal Conductivity and Specific Heat Capacity are calculated based on Latini’s method referred from Sazhin et al. and Rowlinson correlation mentioned in Anand et al respectively [8,46] and tabulated in Table 3.

The binary diffusion coefficient shows a decreasing trend with increasing molar mass which contributes directly to the evaluation of steady evaporation constant and inversely for droplet lifetime. The density of biodiesel shows the exponential increment with molar mass. Coconut recorded the least density (863.2497 kg/m<sup>3</sup>) whereas Radish recorded the highest (870.6853 kg/m<sup>3</sup>) with Madhuca occupying intermediate (867.7161 kg/m<sup>3</sup>). The viscosity shows a decreasing trend with molar mass with negligible variance in thermal conductivity. Figure 1 and Figure 2 show the

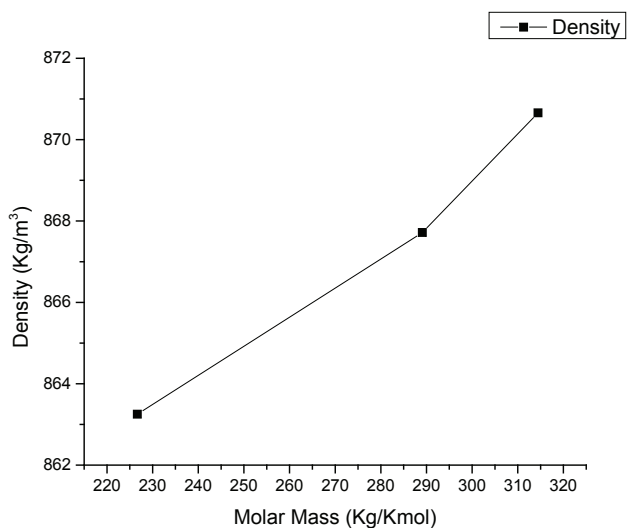


**Figure 1.** Density vs Molar mass.

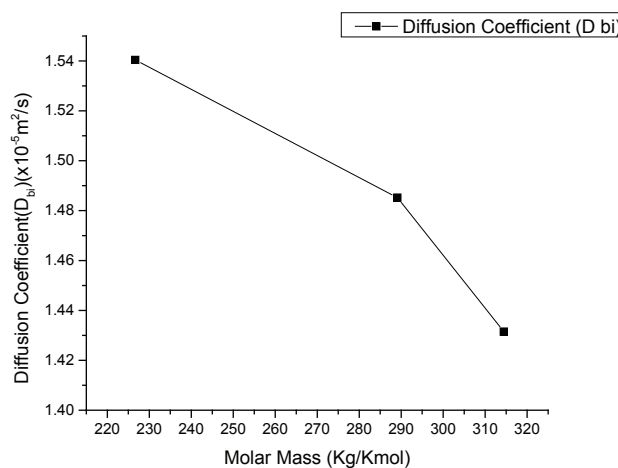


**Figure 2.** Diffusion coefficient vs Molar mass.

variation of liquid density and binary diffusivity concerning molar mass respectively.

**Biodiesel Evaporation**

Critical temperature and critical Pressure are estimated using Joback correlation and Lynderson correlation mentioned in Anand et al. respectively. Similarly Pitzer Correlation mentioned in Anand et al. and Osmont Correlation mentioned in Sazhin et al. were used to determine latent heat of Vaporization and Vapor phase heat capacity. In addition to it Ceraini et al. method is used to calculate Gas Phase Viscosity. Gas phase density was calculated by Ceraini and Mierells method. Boiling point was evaluated using Constantinou and Gani Group contribution method.

In this way estimation of droplet lifetime the thermo-physical properties like Vapour Pressure, Normal Boiling point, Critical temperature, critical pressure, Latent Heat of Vaporization, Fuel Vapour Capacity, Stoichiometric ratio, Gas phase density of vapour air mixture, Gas phase Dynamic viscosity and Dimensionless No. Like Reynold No, Prandtl No, Nusselt No, Transfer No. are calculated using standard theoretical correlations [47–55].

**Expansion lifetime of fuel droplet**

Madhuca oil recorded comparatively higher expansion lifetime (i.e 1.1854 s/mm<sup>2</sup>) than radish oil (i.e 1.1517 s/mm<sup>2</sup>). From our results, we concluded that under the constant heating process the oil with high specific heat capacity requires more heat and hence more time to attain the maximum droplet size during expansion. The volumetric expansion phase shows an increasing trend with thermal conductivity. During the volumetric expansion phase density of oil droplet decreases and its specific volume increases. The expansion curve is non-linear as the slope is continuously changing as the expansion at each instant

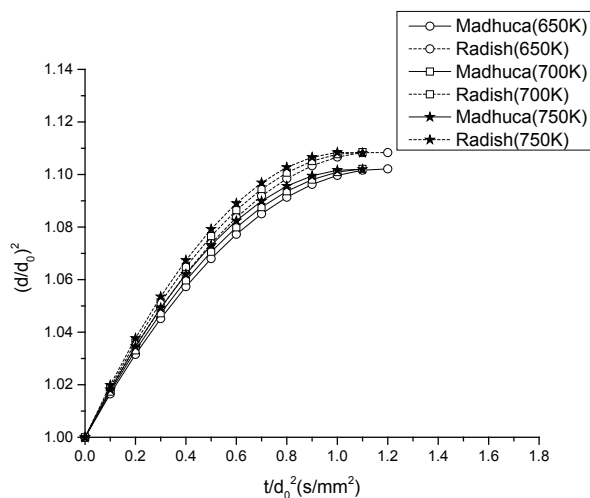


**Figure 3.** Expansion time of fuel droplets at 650K, 700K, and 750K respectively.

of time varies. With the increase in the ambient temperature of the medium, the expansion time for the biodiesel droplets shows a decreasing trend. Generally, the expansion curve converges with the increasing temperature. Expansion droplet lifetime of Radish and Madhuca indica fuels are presented in Figure 3. Generally, the expansion time decreases with increasing temperature for Madhuca oil with the compensation of a decrease in maximum droplet size attained.

Radish oil also follows the same physical phenomenon as Madhuca but the high divergence of the curve with the temperature of Madhuca shows its high sensitiveness to temperature.

Expansion time shows the increase in trend with thermal conductivity because the increase in thermal conductivity increases the thermal conduction and subsequently reduces convection but initially, the heat transfer is maximum through convection, therefore, time required is higher. Expansion time decreases with increase in specific heat capacity generally. Expansion time versus thermal conductivity of coconut, Madhuca, and Radish biodiesel are presented in Figure 4.

**Unsteady evaporation phase of bio-diesel droplet**

Unsteady phase is shortest phase of evaporation. Unsteady time of biodiesel droplet decreases with increasing molar mass due to its capacity to absorb more transient heat within a short interval of time to attain the equilibrium temperature called the wet-bulb temperature. In unsteady phase part of heat from surrounding is used to heat the liquid phase and partly to supply latent heat of vaporization. In Figure 5 Madhuca possess higher unsteady time (i.e., 0.63833 s/mm<sup>2</sup> at 650K) than radish has (i.e., 0.6201 s/mm<sup>2</sup> at 650K) owing to less molar mass comparatively. For different temperature of same oil unsteady time decreases with increasing temperature. The unsteady & expansion time were compared and validated with the Morin et al.,

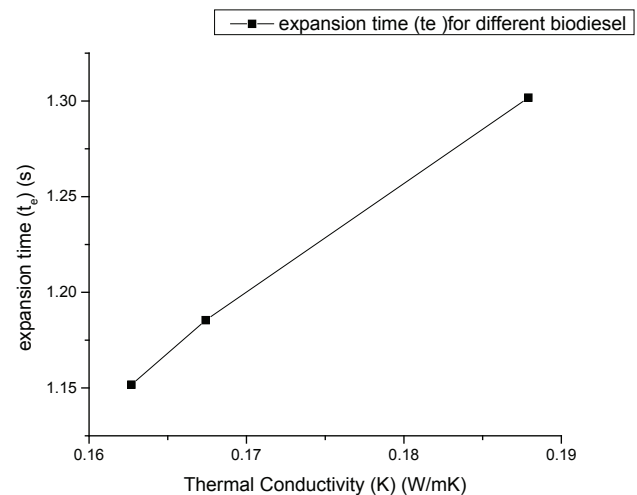


**Figure 4.** Expansion time vs thermal conductivity.

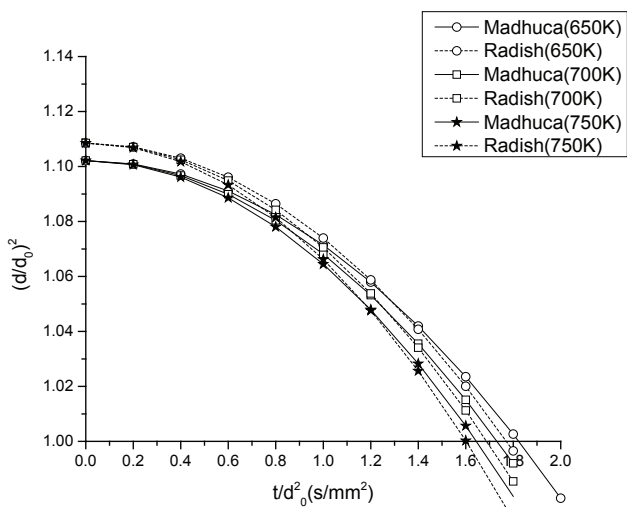


**Figure 5.** Unsteady evaporation phase of bio-diesel droplet at 650K, 700 K, and 750K respectively.

Hasimoto et al. [15,17]. At other temperatures, the oils show the same trend in an unsteady time. The unsteady evaporation curve converges with increasing temperature. The unsteady evaporation curve is non-linear as the slope is continuously changing as the evaporation during this phase is unsteady. The temperature gradient of the unsteady expansion phase is comparatively less for radish oil which signifies its higher insensitiveness to the temperature.

**Steady evaporation time of biodiesel droplet**

Radish oil recorded higher steady-state evaporation lifetime (i.e., 10.23542 s/mm<sup>2</sup> at 650K) than madhuca oil (i.e., 6.81736 s/mm<sup>2</sup> at 650K). The model was created, programmed and validated by inputting the composition values from the Manjunath et al. experiment; the expected error band-width was less than 5%. Since the meagre data was available for the Madhuca Indica & Radish Biodiesel oil, it was confirmed with the Solaimuthu et al. & V.Ravikumar et al. single droplet experimental setup (for reduced pressure) under the acceptable range of error bandwidth [56,57]. The steady-state curve in Figure 6 is linear and converges with an increase in temperature. The high steady time of radish is attributed to its high molar mass, less binary diffusivity, and less evaporation constant value.

**Normalized droplet times of biodiesel droplet evaporation**

From the Figure 7, it is inferred phase 1 (expansion phase) contributes 10-20% of the total lifetime, phase 2 (unsteady evaporation phase) contributes 6-10% of the total life and phase 3 (steady evaporation phase) contributes highest 75-80% of total droplet lifetime. So, the oil with low steady evaporation time owing to its low molar mass, high binary diffusivity, and hence high evaporation constant is more suited for its application in internal combustion engines.

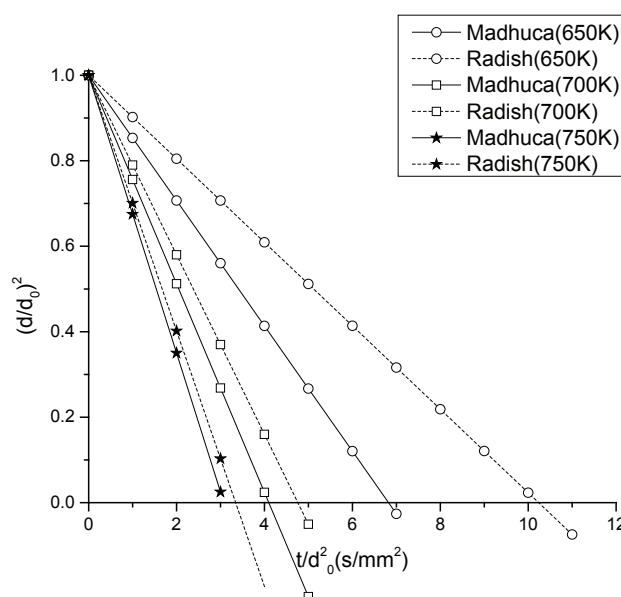


**Figure 6.** Steady evaporation time of biodiesel droplet at 650K, 700K, and 750K respectively.

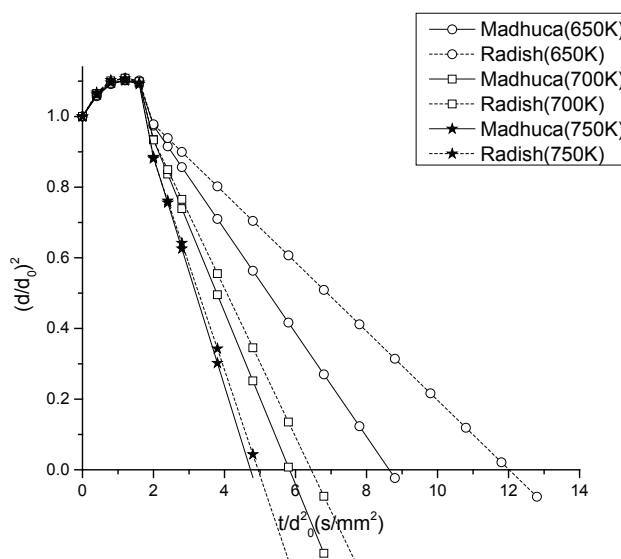


**Figure 7.** Normalized droplet times of biodiesel droplet at 650K,700K and 750K respectively.

The overall evaporation curve seems to converge with increasing temperature. With an increase in temperature the droplet lifetime decreases which provides higher efficiency (decreasing ignition lag) and provides steady combustion (decrease in knocking) upto a certain temperature range after which it shows negligible effect.

Table 4 Volumetric expansion phase as a percentage of total droplet lifetime and volumetric expansion of various biodiesel fuels at different temperatures.



**Table 4.** Percentage of expansion phase for different temperature

Biodiesel	Coconut	Madhuca	Radish
$T_e/T_d$ (650K)	19.96609	13.71899	9.592354
$T_e/T_d$ (700K)	23.39165	19.302728	16.98058
$T_e/T_d$ (750K)	25.58777	22.611033	21.04957
$\% \Delta V$ (650K)	27.66269	32.16645	34.27087

The volume increment is comparatively very less compared to the expansion time for all the oils, where coconut has the highest increment magnitude and Radish with lowest with madhuca occupying the intermediate.

**Steady evaporation time with different Nusselt number**

In our study, we have taken various values of Nusselt number and determined the steady-state lifetime at different temperatures for Madhuca and radish oil shown in Figure 8 and Figure 9. Nusselt number is directly proportional to the steady evaporation constant. It is inferred that the Nusselt number is highest for Clift correlation and the lowest for Chiang correlation. With Haywood, frossling, Faeth, and Lazar occupying 2<sup>nd</sup>, 3<sup>rd</sup> and 4<sup>th</sup> respectively for all temperatures.

The Nusselt number gradient of temperature for each method decreases with an increase in temperature. The variation in steady evaporation time for Radish oil with different Nusselt numbers follows the same trend as Madhuca oil in Figure 10 and Figure 11. The model was created, programmed and validated by inputting the composition values from the Manjunath et al. experiment; the expected error band-with was less than 5%. Since the meagre data was

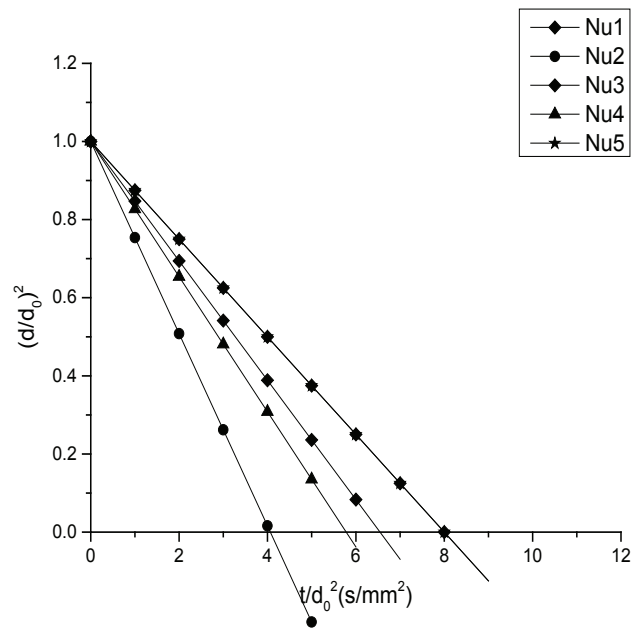


**Figure 9.** Evaporation time of Madhuca oil with different Nusselt numbers at 700K.

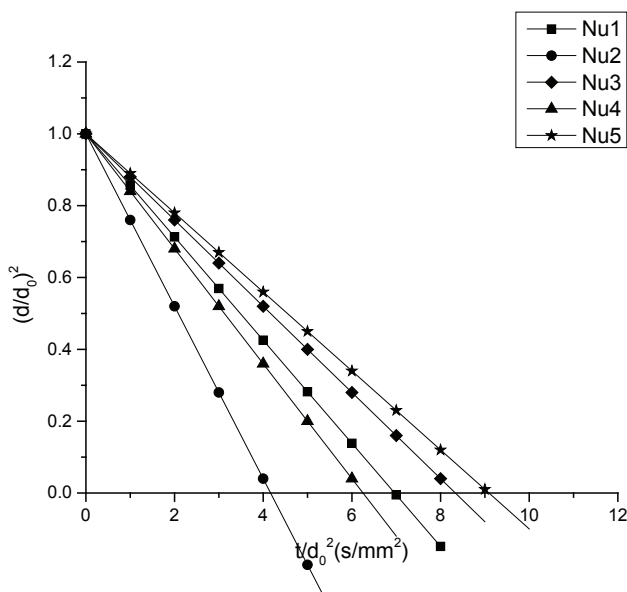


**Figure 8.** Evaporation time of Madhuca oil with different Nusselt numbers at 650K

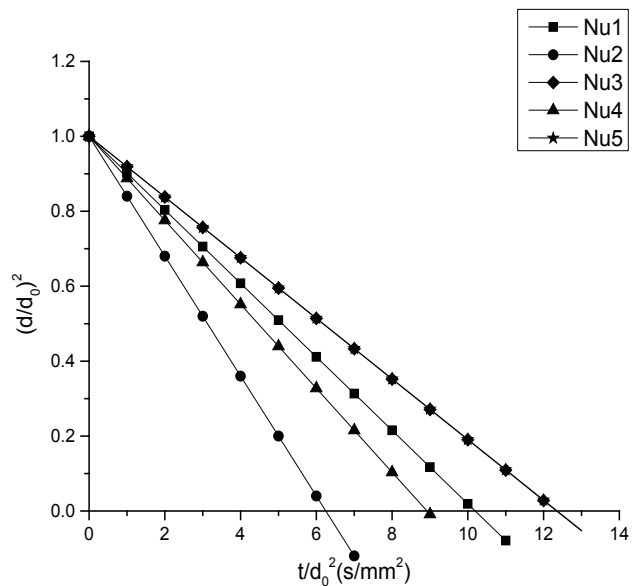


**Figure 10.** Evaporation time of Radish oil with different Nusselt numbers at 650K.

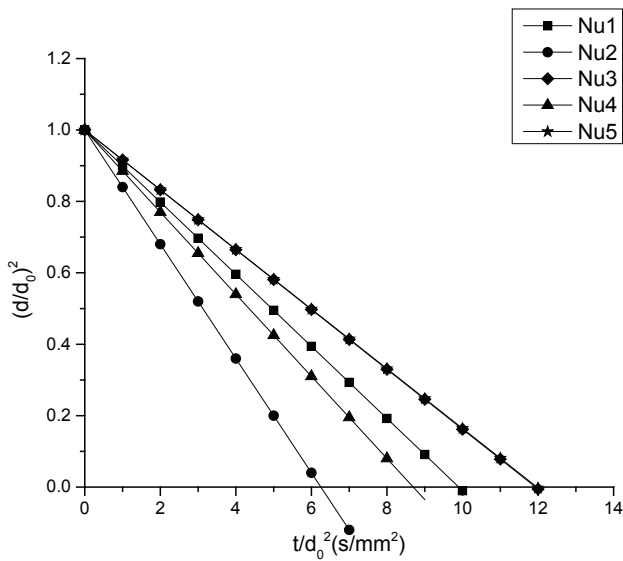


**Figure 11.** Evaporation time of Radish oil with different Nusselt numbers at 700K.

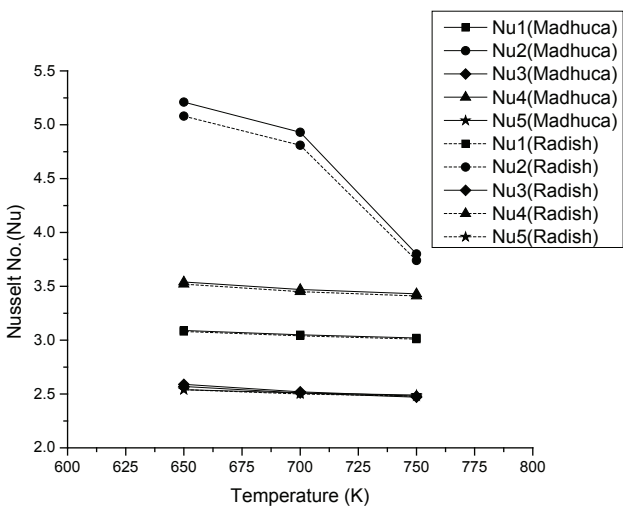


**Figure 12.** Nusselt No. of Madhuca and Radish oil at 650K, 700K and 750K using different correlation.

available for the Madhuca Indica & Radish Biodiesel oil, it was confirmed with the Solaimuthu et al. & V.Ravikumar et al. (for reduced pressure) under the acceptable range of error bandwidth.

## CONCLUSIONS & RECOMMENDATIONS

### Conclusions

Madhuca indica oil superceeds Radish oil due to its high evaporation & burning constant owing to its low molar mass, and high binary diffusivity leading to a less normalized droplet lifetime reducing the charge accumulation complexity

thus eliminating knocking. Radish oil excels the Madhuca in the atomization characteristics crucial parameter in spray combustion due to its low viscosity thus reducing the detonation. The low droplet evaporation & burning lifetime of the Madhuca under stagnant conditions surpass Radish for its applicability in the gravity-free zone (space-shuttle & permanent space station in low earth orbit). Also its high evaporation constant value finds vast applicability in the spray combustion in modified IC engine performance optimization under its usage after emulsification & blending with additive and the reduction in emission characteristics. The burning characteristics analysis aid in predicting the selectivity of fuel in the specified combustion modeling for the devices.

### Recommendations

The Stefan problem being reduced to spherical symmetry should be further reduced to the axis-symmetric problem. Species, mass, heat conservation & transport analysis should be carried out instantaneously using combined heat & mass transfer equations. The effects of internal circulation (shear-driven fluid motion with droplet), soot shell formation, fuel-vapor accumulation & interaction among multiple droplets should be taken into account for the exact simulation of fuel characteristics. Consideration of supercritical droplet combustion and evaporation should be introduced for its applicability in diesel and rocket engines.

## NOMENCLATURE

$C_{pl}$	Liquid Phase Specific heat Capacity
$\rho_l$	Liquid Phase Density
$C_{pg}$	Gas Phase Heat Capacity
$d_h$	Average droplet Diameter During Heating
$T_s$	Droplet Surface temperature
$T_{s0}$	Initial Droplet surface Temperature
$\lambda_g, K_g$	Gas Phase Thermal Conductivity
$B_{Th}$	Thermal transfer number
$B_{Mh}$	Mass Transfer Number
$L_{vh}$	Latent Heat of Vaporization at Vapour Phase
$T_\infty$	Ambient Temperature
$Y_{Fs}$	Mass fraction of fuel vapour
$T_{nb}$	Normal Boiling Temperature
$T_c$	Critical Temperature
$L_v$	Latent Heat at Vapour Phase
$L_{Tnb}$	Latent Heat at Normal boilingPoint
$\dot{m}$	Total mass evaporation rate
$\dot{m}_F$	Fuel mass evaporation rate
$\rho$	Density at Gas Phase
$v_r$	Bulk flow Velocity
$r$	Droplet radius
$D$	Mass Diffusivity
$h_{f,i}$	Enthalpy of fuel droplet interior region
$K$	Thermal Conductivity
$Q_{cand}$	Heat Through Conduction
$h_{vap}$	Enthalpy of Vapour
$h_{liq}$	Enthalpy of Liquid

$h_{fg}$	Sensible Heat Exchange
$T_{boil}$	Boiling Point Temperature
$B_q, B_{o,q}$	Transfer number of Heat
$Nu$	Nusselt Number
$D_{bi}$	Binary Diffusivity
$K_{evp,s}$	Steady Evaporation rate
$D$	Droplet Diameter
$D_0$	Initial Droplet Diameter
$t_d$	Droplet lifetime
$C_{PF}$	Specific Heat Capacity of Fuel
$K_f$	Thermal Conductivity of Fuel Vapour
$\bar{T}$	Mean Temperature of Fuel & A
$Re_d$	Reynold No of Air flow over Droplet
$Pr_g$	Prandtl number of gas
$U_{rel}$	Relative velocity of air over Droplet
$\omega$	Accentric Factor

## AUTHORSHIP CONTRIBUTIONS

Authors equally contributed to this work.

## DATA AVAILABILITY STATEMENT

The authors confirm that the data that supports the findings of this study are available within the article. Raw data that support the finding of this study are available from the corresponding author, upon reasonable request.

## CONFLICT OF INTEREST

The author declared no potential conflicts of interest with respect to the research, authorship, and/or publication of this article.

## ETHICS

There are no ethical issues with the publication of this manuscript.

## REFERENCES

- [1] Lapuerta M, Armas O, Rodríguez-Fernández J. Effect of biodiesel fuels on diesel engine emissions. *Prog Energy Combust Sci* 2008;34:198–223. [\[CrossRef\]](#)
- [2] Sharma YC, Singh B, Upadhyay SN. Advancements in development and characterization of biodiesel: A review. *Fuel* 2008;87:2355–2373. [\[CrossRef\]](#)
- [3] Vyas AP, Verma JL, Subrahmanyam N. A review on FAME production processes. *Fuel* 2010;89:1–9. [\[CrossRef\]](#)
- [4] Sinha S, Agarwal AK, Garg S. Biodiesel development from rice bran oil: Transesterification process optimization and fuel characterization. *Energy Convers Manag* 2008;49:1248–1257. [\[CrossRef\]](#)
- [5] Manjunath M, Prakash P, Raghavan V, Mehta PS. Composition Effects on Thermo-Physical Properties and Evaporation of Suspended Droplets of Biodiesel Fuels. *SAE Int J Fuels Lubr* 2014;7:833–841. [\[CrossRef\]](#)
- [6] Arabkhalaj A, Azimi A, Ghassemi H, Shahsavan Markadeh R. A fully transient approach on evaporation of multi-component droplets. *Appl Therm Eng* 2017;125:584–595. [\[CrossRef\]](#)
- [7] Dirbude S, Eswaran V, Kushari A. Droplet vaporization modeling of rapeseed and sunflower methyl esters. *Fuel* 2012;92:171–179. [\[CrossRef\]](#)
- [8] Al Qubeissi M, Sazhin S, Crua C, Heikal MR. ICHTA 2015: International Conference on Heat Transfer and Applications, World Academy of Science Engineering and Technology (WASET). 2015 January; London: International Scholarly and Scientific Research & Innovation; 2015. pp. 46–49.
- [9] Golovitchev VI, Yang J. Construction of combustion models for rapeseed methyl ester bio-diesel fuel for internal combustion engine applications. *Biotechnol Adv* 2009;27:641–655. [\[CrossRef\]](#)
- [10] Lakhfif F, Nemouchi Z, Mebarek-Oudina F. Numerical Investigation of the Different Spray Combustion Models under Diesel Condition. *Int J Appl Eng Res* 2016;11:9393–9399.
- [11] Al Qubeissi M, Sazhin SS, Elwardany AE. Modelling of blended Diesel and biodiesel fuel droplet heating and evaporation. *Fuel* 2017;187:349–355. [\[CrossRef\]](#)
- [12] Lasheras JC, Fernandez-Pello AC, Dryer FL. On the disruptive burning of free droplets of alcohol/n-paraffin solutions and emulsions. *Symp Combust* 1981;18:293–305. [\[CrossRef\]](#)
- [13] Hallett WLH, Beauchamp-Kiss S. Evaporation of single droplets of ethanol-fuel oil mixtures. *Fuel* 2010;89:2496–2504. [\[CrossRef\]](#)
- [14] Hallett WLH, Legault NV. Modelling biodiesel droplet evaporation using continuous thermodynamics. *Fuel* 2011;90:1221–1228. [\[CrossRef\]](#)
- [15] Morin C, Chauveau C, Gökalp I. Droplet vaporisation characteristics of vegetable oil derived bio-fuels at high temperatures. *Exp Therm Fluid Sci* 2000;21:41–50. [\[CrossRef\]](#)
- [16] Daho T, Vaitilingom G, Sanogo O, Ouiminga SK, Segda BG, Valette J, et al. Model for predicting evaporation characteristics of vegetable oils droplets based on their fatty acid composition. *Int J Heat Mass Transf* 2012;55:2864–2871. [\[CrossRef\]](#)
- [17] Hashimoto N, Nomura H, Suzuki M, Matsumoto T, Nishida H, Ozawa Y. Evaporation characteristics of a palm methyl ester droplet at high ambient temperatures. *Fuel* 2015;143:202–210. [\[CrossRef\]](#)
- [18] Hołyst R, Litniewski M, Jakubczyk D, Kolwas K, Kolwas M, Kowalski K, et al. Evaporation of freely suspended single droplets: Experimental, theoretical and computational simulations. *Rep Prog Phys* 2013;76:3. [\[CrossRef\]](#)
- [19] Gautam A, Agarwal AK. Determination of important biodiesel properties based on fuel temperature correlations for application in a locomotive engine. *Fuel* 2015;142:289–302. [\[CrossRef\]](#)

- [20] Turns S. An Introduction to combustion. 2nd ed. New York: McGraw Hill; 1996.
- [21] Nishiwaki N. Kinetics of liquid combustion processes: Evaporation and ignition lag of fuel droplets. *Symp Combust* 1955;5:148–158. [CrossRef]
- [22] Law CK, Williams FA. Kinetics and convection in the combustion of alkane droplets. *Combust Flame* 1972;19:393–405. [CrossRef]
- [23] Froessling N. Über die Verdunstung fallender Tropfen. *Mater Sci* 1938;52:170–216.
- [24] Ranz WE, Marshall WR. Evaporation from drops. *Chem Eng Prog* 1952;48:146.
- [25] Ranz WE, Marshall wr. Evaporation from drops. *Chem Eng Prog* 1952;48:173–180.
- [26] Clift R, Grace JR, Weber ME. Bubbles, Drops, and Particles. New York: Academic Press; 1978.
- [27] Faeth GM, Lazar RS. Fuel droplet burning rates in a combustion gas environment. *AIAA J* 1971;9:2165–2171. [CrossRef]
- [28] Haywood RJ, Nafziger R, Renksizbulut M. A detailed examination of gas and liquid phase transient processes in convective droplet evaporation. *J Heat Transf* 1989;111:495–502. [CrossRef]
- [29] Chiang CH, Raju MS, Sirignano WA. Numerical analysis of convecting, vaporizing fuel droplet with variable properties. *Int J Heat Mass Transf* 1992;35:1307–1324. [CrossRef]
- [30] N.C. WebBook, <https://webbook.nist.gov/chemistry/>. Accessed on Nov 20, 2023.
- [31] Clean Fuels Alliance America N.B.B. Available at: <https://www.biodiesel.org/> Accessed on Nov 20, 2023.
- [32] Researchgate. Available at: <https://www.researchgate.net/> Accessed on Nov 20, 2023.
- [33] Barabas I, Todorut A. Biodiesel Quality Standards Properties. In: Montero G, Stoytcheva M, editors. *Biodiesel-Quality, Emissions and By-Product*. 1 ed. London: In Tech Open; 2011.
- [34] Cunico LP, Ceriani R, Guirardello R. Estimation of physical properties of vegetable oils and biodiesel using group contribution methods. *Chem Eng Trans* 2013;32:535–540.
- [35] Ruan DF, Chen ZH, Wang KF, Chen Y, Yang F. Physical Property Prediction for Waste Cooking Oil Biodiesel. *Open Fuels Energy Sci J* 2014;7:62–68. [CrossRef]
- [36] Freitas SVD, Pratas MJ, Ceriani R, Lima AS, Coutinho JAP. Evaluation of predictive models for the viscosity of biodiesel. *Energy and Fuels* 2011;25:352–358. [CrossRef]
- [37] Krisnangkura K, Yimsuwan T, Pairintra R. An empirical approach in predicting biodiesel viscosity at various temperatures. *Fuel* 2006;85:107–113. [CrossRef]
- [38] An H, Yang WM, Maghbouli A, Chou SK, Chua KJ. Detailed physical properties prediction of pure methyl esters for biodiesel combustion modeling. *Appl Energy* 2013;102:647–656. [CrossRef]
- [39] Perry RH, Green DW. Sec. 22: Membrane Separation Processes, 1997. Available at: <http://pubs.acs.org/doi/pdf/10.1021/ed027p533.1> Accessed on Nov 20, 2023.
- [40] Oertel H. Properties of Liquids and Gases. *Appl Math Sci* 2010;158:15–42. [CrossRef]
- [41] Tesfa B, Mishra R, Gu F, Powles N. Prediction models for density and viscosity of biodiesel and their effects on fuel supply system in CI engines. *Renew Energy* 2010;35:2752–2760. [CrossRef]
- [42] Mesquita FMR, Feitosa FX, Do Carmo FR, De Santiago-Aguiar RS, De Sant'ana HB. Viscosities and viscosity deviations of binary mixtures of biodiesel + petrodiesel (or n-hexadecane) at different temperatures. *Brazilian J Chem Eng* 2012;29:653–664. [CrossRef]
- [43] Prieto NMCT, Ferreira AGM, Portugal ATG, Moreira RJ, Santos JB. Correlation and prediction of biodiesel density for extended ranges of temperature and pressure. 2014;8:1285–1294. <https://waset.org/publications/10000012/correlation-and-prediction-of-biodiesel-density>.
- [44] Saxena P, Joshipura MH. Prediction of Density of Fatty Acid Alkyl Esters (Biodiesel) by Various Group- Contributioan Methods; 56–58.
- [45] Pratas MJ, Freitas SVD, Oliveira MB, Monteiro SC, Lima AS, Coutinho JAP. Biodiesel density: Experimental measurements and prediction models. *Energy Fuels* 2011;25:2333–2340. [CrossRef]
- [46] Sazhin SS, Al Qubeissi M, Kolodnytska R, Elwardany AE, Nasiri R, Heikal MR. Modelling of biodiesel fuel droplet heating and evaporation. *Fuel* 2014;115:559–572. [CrossRef]
- [47] Yuan W, Hansen AC, Zhang Q. Vapor pressure and normal boiling point predictions for pure methyl esters and biodiesel fuels. *Fuel* 2005;84:943–950. [CrossRef]
- [48] Constantinou L, Gani R. New group contribution method for estimating properties of pure compounds. *AIChE J* 1994;40:1697–1710. [CrossRef]
- [49] García Santander CM, Gómez Rueda SM, De Lima Da Silva N, De Camargo CL, Kieckbusch TG, Wolf MacIel MR. Measurements of normal boiling points of fatty acid ethyl esters and triacylglycerols by thermogravimetric analysis. *Fuel* 2012;92:158–161. [CrossRef]
- [50] Neto EGL, Silva GP, Silva GF. Evaluation of Group-Contribution Methods to Estimate Vegetable Oils and Biodiesel Properties. *Int J Eng Technol* 2012;2:1600–1605.
- [51] Su YC, Liu YA, Diaz Tovar CA, Gani R. Selection of prediction methods for thermophysical properties for process modeling and product design of biodiesel manufacturing. *Ind Eng Chem Res* 2011;50:6809–6836. [CrossRef]
- [52] Díaz OC, Schoeggl F, Yarranton HW, Satyro MA. Equation of state modeling for the vapor pressure of biodiesel fuels. *Fluid Phase Equilib* 2015;389:55–63. [CrossRef]

- 
- [53] Owczarek I, Blazej K. Recommended critical pressures. Part I. Aliphatic hydrocarbons. *J Phys Chem Ref Data* 2006;35:1461–1474. [\[CrossRef\]](#)
- [54] Ro PS, Fahlen TS, Bryant HC. Precision Measurements of Water Droplet Evaporation Rates. *Appl Opt* 1968;7:883. [\[CrossRef\]](#)
- [55] Sinha A, Surya Prakash R, Mohan AM, Ravikrishna RV. Experimental studies on evaporation of fuel droplets under forced convection using spray in crossflow methodology. *Fuel* 2016;164:374–385. [\[CrossRef\]](#)
- [56] Ravikumar V, Senthilkumar D, Solaimuthu C. Evaporation rate and engine performance analysis of coated diesel engine using *Raphanus sativus* biodiesel and its diesel blends. *Int J Ambient Energy* 2017;38:202–208. [\[CrossRef\]](#)
- [57] Solaimuthu C, Senthilkumar D, Ramasamy KK. An experimental investigation of performance, combustion and emission characteristics of mahua (*Madhuca Indica*) oil methyl ester on four-stroke direct injection diesel engine. *Indian J Eng Mater Sci* 2013;20:42–50.